

Detection of Myocardial Infarction From 12-Lead ECG Trace Images Using Eigendomain Deep Representation Learning

Sathvik Bhaskarpandit^{ID}, *Student Member, IEEE*, Anurag Gade^{ID}, Shaswati Dash^{ID}, Dinesh Kumar Dash^{ID}, *Member, IEEE*, Rajesh Kumar Tripathy^{ID}, *Member, IEEE*, and Ram Bilas Pachori^{ID}, *Senior Member, IEEE*

Abstract— Myocardial infarction (MI) is a life-debilitating emergency in which there is a lack of blood flow in the heart muscle, resulting in permanent damage to the myocardium and sudden cardiac death. The 12-lead electrocardiogram (ECG) is a standardized diagnostic test conducted in hospitals to detect and localize MI-based heart disease. To diagnose MI, the cardiologist visualizes the alternations in the patterns of the 12-lead-based ECG trace image. The automated detection of MI from the 12-lead-based ECG trace image using artificial intelligence (AI)-based approaches is important in the clinical study for the accurate diagnosis of MI disease. This article proposes a novel eigendomain-based deep representation learning (DRL) approach to automatically detect MI using 12-lead ECG trace images. The singular value decomposition (SVD) and eigendomain grouping are used to evaluate five modes or components from the 12-lead ECG trace image. The EfficientNetV2B2-based transfer learning model extracts feature maps from the 12-lead ECG trace image and all five modes. The global average pooling (GAP), batch normalization (BN), dropout, and soft-max layers are used for each feature map to obtain the probability scores. The concatenated probability scores of all the feature maps, followed by the dense layer and output layer, are used to detect MI. A public database containing the 12-lead ECG trace images is used to evaluate the performance of the proposed approach. The results show that for the MI class, the proposed approach has achieved the accuracy value of 100%. Similarly, for normal versus MI versus other cardiac-arrhythmia-based disease classification schemes, the proposed approach has obtained the overall accuracy, F1-score, specificity, and sensitivity values of 99.03%, 99.01%, 99.49%, and 98.96%, respectively using fivefold cross-validation (CV). The suggested approach has demonstrated higher overall accuracy than 24 existing transfer-learning-based models to detect MI using the 12-lead ECG trace images.

Index Terms— 12-Lead electrocardiogram (ECG) trace image, deep learning (DL), eigendomain analysis, myocardial infarction (MI), performance evaluation.

Manuscript received 24 September 2022; revised 26 December 2022; accepted 20 January 2023. Date of publication 3 February 2023; date of current version 13 February 2023. The Associate Editor coordinating the review process was Dr. Chengyu Liu. (*Sathvik Bhaskarpandit and Anurag Gade contributed equally to this work.*) (*Corresponding author: Rajesh Kumar Tripathy.*)

Sathvik Bhaskarpandit, Anurag Gade, Shaswati Dash, and Rajesh Kumar Tripathy are with the Department of EEE, BITS-Pilani, Hyderabad Campus, Hyderabad 500078, India (e-mail: rajeshiitg13@gmail.com).

Dinesh Kumar Dash is with the Department of Electronics and Telecommunication Engineering, Parala Maharaja Engineering College, Berhampur 761003, India (e-mail: dinesh.etc@pmec.ac.in).

Ram Bilas Pachori is with the Department of Electrical Engineering, Indian Institute of Technology Indore, Indore 453552, India (e-mail: pachori@iiti.ac.in).

Digital Object Identifier 10.1109/TIM.2023.3241986

I. INTRODUCTION

MYOCARDIAL infarction (MI) is a life-threatening cardiac condition where the heart muscle does not receive sufficient blood and, as a result, begins to die [1]. This usually happens due to the formation of atherosclerosis plaque in the coronary arteries, which further blocks the blood flow [2]. The MI disease usually progresses in phases like acute, ischemic, and necrosis [3], [4]. The 12-lead electrocardiogram (ECG) test is conducted in the clinical scenario for the early detection of this cardiac ailment [2]. Typically, the 12-lead ECG printout or ECG trace image generated after the test is to be submitted to the physicians for the diagnosis of MI [5]. The physician typically checks the changes in the morphological patterns such as ST-segment, RR-duration, QRS-complex, and T-wave to diagnose MI disease [6], [7]. ECG trace images are frequently taken for critical patients to diagnose different cardiac ailments [8]. Hence, it is cumbersome for physicians to manually visualize all the ECG trace images for diagnosing MI disease, which may lead to diagnosis errors. Hence, the automated analysis of ECG trace images using different artificial intelligence (AI)-based techniques is required to detect MI heart ailment accurately. The AI-based techniques use either machine learning (ML) or deep learning (DL)-based models for automated detection of MI using 12-lead ECG data [2], [9]. The DL-based MI detection models do not rely on the requirements such as extraction of raw features from 12-lead ECG signals, selection of relevant features, and classifiers for MI detection [9]. These models can be constructed using trainable and nontrainable layers [10]. For trainable layers, the parameters, such as the weight matrix and bias vector, are updated at each epoch in the training phase of the model. However, in the nontrainable layers, the parameters from the transfer learning models are used, and these parameters are not updated in the training of the DL model [11]. The DL model with fewer trainable parameters helps reduce the utilization of resources and time during training [10]. Therefore, developing a DL model with few trainable parameters is required for automated detection of MI disease using the 12-lead ECG trace images.

In recent years, different AI-based approaches have been used to automatically detect MI and other diseases using ECG trace images. Sane et al. [5], have considered an

11-layer-based deep convolutional neural network (CNN) framework to detect MI using the 12-lead ECG trace images and obtained an overall accuracy value of 86.21%. Similarly, Mhamdi et al. [12] have used fine-tuned MobileNet V2 and VGG16 transfer learning models to detect MI and other cardiac diseases using the 12-lead ECG trace images. They have reported accuracy values of 91% and 95% using fine-tuned MobileNetV2 and VGG16 models. Moreover, various DL models such as CNN [13], transfer learning domain bilevel feature fusion network [14], and transfer learning models such as ResNet, InceptionNetV3, and DenseNet201 [15] have been used for automated classification of the 12-lead ECG trace images. The methods reported above [13], [14], [15] have mainly focused on the automated detection of coronavirus disease 2019 (COVID-19) using DL with ECG trace images. Only limited work has been reported in the literature to detect MI and other cardiac ailments using the 12-lead ECG trace images. Furthermore, the methods in [5] and [12] have demonstrated less classification performance and have high trainable parameters for detecting MI using ECG trace images. Therefore, an automated DL-based approach with less trainable parameters can be developed to detect MI and other cardiac diseases using the 12-lead ECG trace images.

The existing DL-based models have considered direct 12-lead ECG trace image as input for automated detection of MI ailment. The multiscale domain DL (MDDL) model has been recently proposed for the analysis and classification of X-ray images [16]. In the MDDL model, empirical wavelet transform (EWT) decomposes the X-ray image into modes or interpretable components. Then, the DL model is developed by considering the modes of X-ray images [16]. The transfer-learning-based nontrainable layers can be used in the multiscale domain or modes of the medical image for automated pathology detection. The motivation of this study is to develop a multiscale domain representation learning model by considering the eigendecomposition-based multiscale analysis of the 12-lead ECG trace images and transfer learning for automated detection of MI. The eigenanalysis based on singular value decomposition (SVD) is used to factorize a matrix into the eigenmatrices and singular value matrix [17]. It is a data-driven multiscale analysis technique to extract the local information or components of the image based on the grouping of the eigentriples (eigenmatrices and singular values) [18]. The 12-lead ECG trace images can be decomposed into components or modes based on eigenanalysis. Similarly, deep representation learning (DRL) is a technique in which each layer of the network transforms the input data or feature maps into a new domain for classification and prediction applications [19], [20]. The eigenanalysis domain DRL has not been explored to analyze the 12-lead ECG trace images. The novelty of this work is to develop a novel approach for automated detection of MI and other cardiac ailments using the 12-lead ECG trace images. The essential contributions of this work are given as follows.

- 1) The eigenanalysis-based approach is used to evaluate the modes from the 12-lead ECG trace images.

- 2) The modes or the components of the 12-lead ECG trace images coupled with the DRL framework are used to detect MI.
- 3) The classification performance of the DRL based on EfficientNetV2B2 is compared with DRL based on ResNet50, DRL based on InceptionV3, DRL based on VGG16, and DRL based on DenseNet121 for MI detection.
- 4) The proposed approach is also compared with 24 transfer-learning-based models for detecting MI using the 12-lead ECG trace images.

The remaining parts of this article can be organized as follows. In Section II, we have described the details of the 12-lead ECG trace image database. Similarly, the theoretical details of the proposed eigendomain DRL approach are outlined in Section III. Moreover, the obtained results of the proposed approach and the discussion regarding the results are presented in Section IV. Finally, we have presented the conclusions of this article in Section V.

II. 12-LEAD ECG TRACE IMAGE DATABASE

The 12-lead ECG trace images used in this work are taken from a publicly available database in the Mendeley data source [21]. This database consists of the 12-lead ECG trace images from 240 MI, 284 normal, and 233 abnormal heartbeats or other cardiac-ailment-based subjects. Similarly, it also contains the 12-lead ECG trace images from 172 subjects with a history of MI pathology. The sampling frequency of the signals is 500 Hz for each 12-lead ECG trace image. The senior medical professionals have given the annotations of 12-lead ECG recordings. We have considered all the 12-lead ECG trace images from normal, MI, and other cardiac ailments' categories to develop the proposed eigendomain DRL model. The 12-lead ECG trace image format is different for different hospitals. To verify the robustness of the proposed approach, we have used different format-based 12-lead ECG trace images for MI detection. For that, the 12-lead ECG recordings from 73 healthy (normal) and 100 MI cases are collected from the Physikalisch-Technische Bundesanstalt (PTB) diagnostic database [22], [23]. The sampling frequency of each 12-lead ECG recording is 1000 Hz. The first 25-s duration of 12-lead ECG recordings from normal and MI classes is used in this work. We have applied a Butterworth high-pass filter of 0.5 Hz to remove the baseline wandering artifacts from 12-lead ECG recordings from the PTB database [2]. The filtered 12-lead ECG recordings are segmented into frames using a nonoverlapping window of duration 5 s (5000 samples). After segmentation, the size of the 12-lead ECG frame is given by 12×5000 . The ECG-plot-based python library [24] is used to generate a 12-lead ECG trace image from the 12-lead ECG frame of size 12×5000 . In this work, we have evaluated 500 MI and 365 normal-based 12-lead ECG trace images from the PTB database 12-lead ECG recordings to evaluate the proposed approach.

III. PROPOSED APPROACH

The flowchart of the proposed eigendomain DRL framework is depicted in Fig. 1. It consists of preprocessing the 12-lead

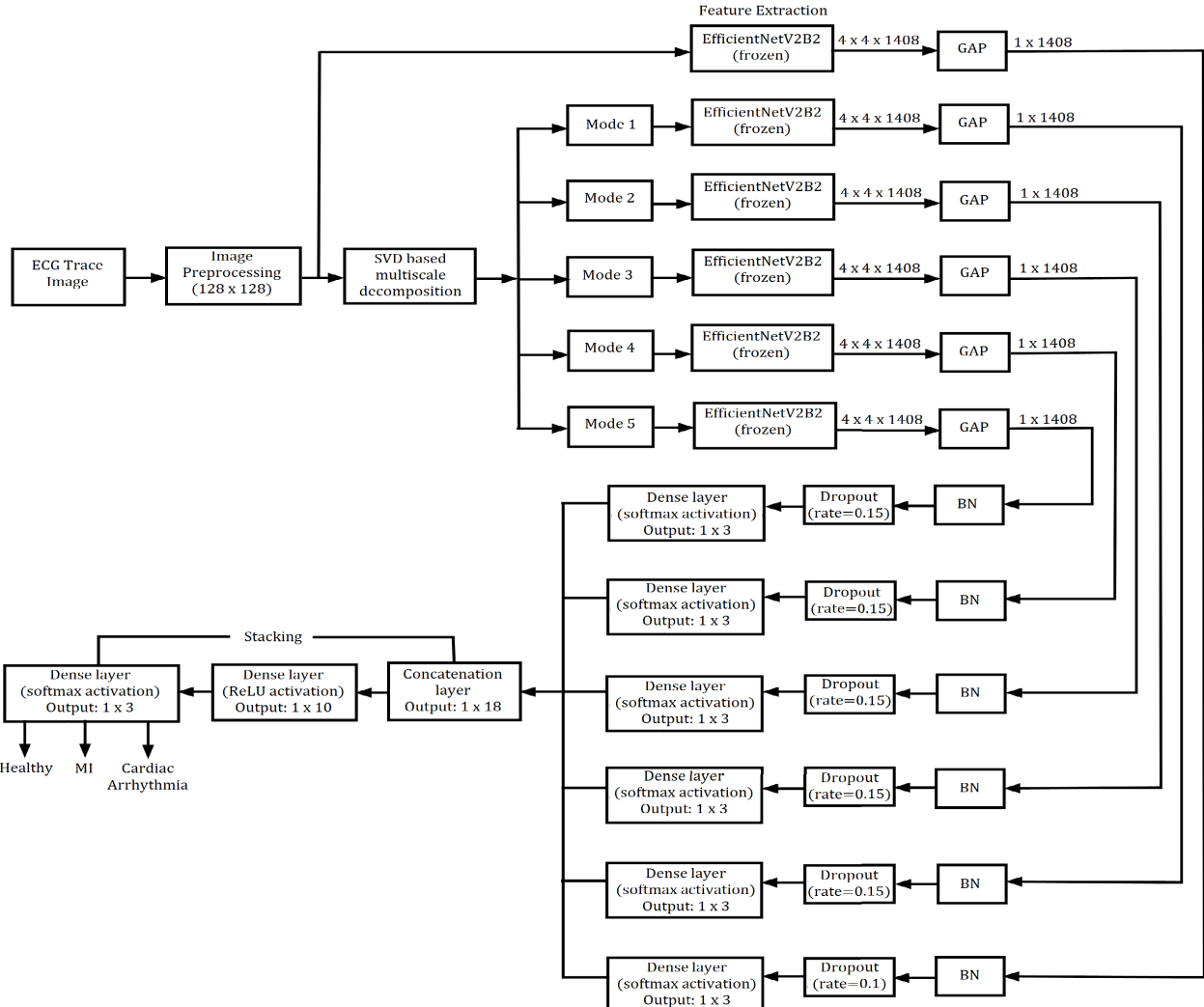


Fig. 1. Flowchart of the proposed eigendomain DRL approach to detect MI using ECG trace images.

ECG trace image and multiscale decomposition of the 12-lead ECG trace image into modes using SVD and modal domain DRL. In Sections III-A–III-C, we have written a detailed description of each block in Fig. 1.

A. Preprocessing of 12-Lead ECG Trace Image

In the database, the 12-lead ECG trace image contains texts such as titles and other words for diagnosing cardiac diseases. The texts and white spaces are identical for all the 12-lead ECG trace images of different classes. Hence, their presence would not improve the classification performance of the proposed eigendomain DRL model for MI detection. In this work, we have cropped each of the 12-lead ECG trace images using the concept of array slicing, which removes the text from the 12-lead ECG trace images. The preprocessing part also includes resizing a 12-lead ECG trace image into a color 12-lead ECG trace image of size [128, 128, 3]. Furthermore, the resized color 12-lead ECG trace image is converted into a grayscale image, and the size of the 12-lead ECG grayscale trace image is [128, 128]. This grayscale 12-lead ECG trace image is used as the input to SVD for multiscale decomposition and evaluation of modes.

B. Eigendecomposition of 12-Lead ECG Trace Image

The grayscale 12-lead ECG image is represented in matrix form as $\mathbf{X} \in \mathbb{R}^{128 \times 128}$. The SVD of the matrix \mathbf{X} produces three submatrices, and it is given as follows [17]:

$$\mathbf{X} = \mathbf{U}\mathbf{S}\mathbf{V}^T \quad (1)$$

where \mathbf{U} and \mathbf{V} stand for the left eigenmatrix and right eigenmatrix of the 12-lead ECG trace image, respectively. \mathbf{S} is a diagonal matrix containing the singular values. The singular value vector (d) evaluated from the \mathbf{S} matrix using diagonalization is given by [18]

$$d = \text{diag}(\mathbf{S}). \quad (2)$$

The grayscale 12-lead ECG trace images for normal, MI, and other cardiac ailments are depicted in Fig. 2(a)–(c), respectively. Similarly, we have shown different format-based 12-lead ECG trace images evaluated from the PTB database ECG signals in Fig. 3(a) and (b), respectively, for normal and MI classes. It is noted that the 12-lead ECG trace images have different morphological changes for normal, MI, and other cardiac ailment classes. The local information or modes

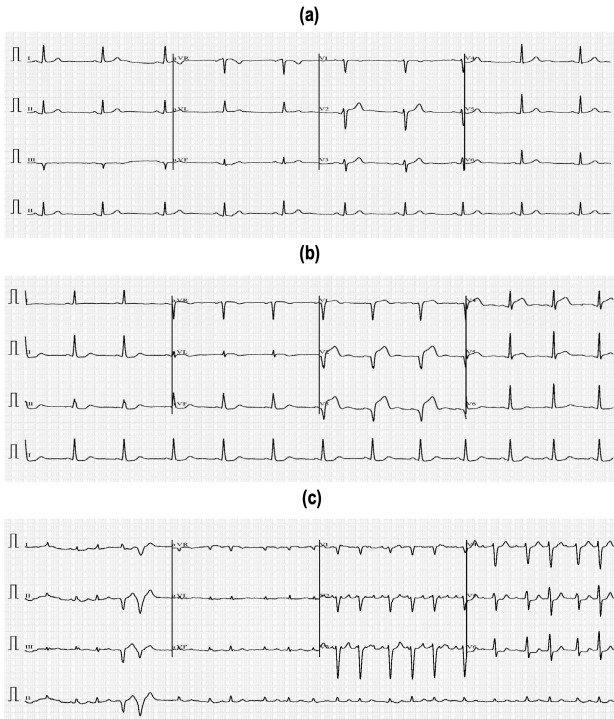


Fig. 2. (a) 12-Lead ECG trace image for normal class, (b) 12-lead ECG trace image for MI class, and (c) 12-lead ECG trace image for other cardiac ailment class.

evaluated from the SVD-based analysis of the 12-lead ECG trace images can be used for automated detection of MI and other cardiac ailments. In this work, five modes are computed from the 12-lead ECG trace images of each class. Mode 1 is evaluated by considering the first five singular values and the first five eigenvectors from \mathbf{U} and \mathbf{V} matrices, respectively. Therefore, mode 1 image (\mathbf{M}_1) is evaluated as follows:

$$\mathbf{M}_1 = \tilde{\mathbf{U}}_1 \tilde{\mathbf{S}}_1 \tilde{\mathbf{V}}_1^T \quad (3)$$

where $\tilde{\mathbf{U}}_1 = \mathbf{U}(:, (1 : 5))$, $\tilde{\mathbf{V}}_1 = \mathbf{V}(:, (1 : 5))$, and $\tilde{\mathbf{S}}_1 = \mathbf{S}(:, (1 : 5))$ are the left eigenmatrix, right eigenmatrix, and singular value matrix for the first five eigentriples, respectively. Similarly, mode 2 of the 12-lead ECG trace image is computed as follows:

$$\mathbf{M}_2 = \tilde{\mathbf{U}}_2 \tilde{\mathbf{S}}_2 \tilde{\mathbf{V}}_2^T \quad (4)$$

where $\tilde{\mathbf{U}}_2 = \mathbf{U}(:, (6 : 15))$, $\tilde{\mathbf{V}}_2 = \mathbf{V}(:, (6 : 15))$, and $\tilde{\mathbf{S}}_2 = \mathbf{S}(:, (6 : 15), (6 : 15))$ are the matrices for 6th to 15th eigentriples. Furthermore, mode 3 of the 12-lead ECG trace image is evaluated using the following equation:

$$\mathbf{M}_3 = \tilde{\mathbf{U}}_3 \tilde{\mathbf{S}}_3 \tilde{\mathbf{V}}_3^T \quad (5)$$

where $\tilde{\mathbf{U}}_3 = \mathbf{U}(:, (16 : 25))$, $\tilde{\mathbf{V}}_3 = \mathbf{V}(:, (16 : 25))$, and $\tilde{\mathbf{S}}_3 = \mathbf{S}(:, (16 : 25), (16 : 25))$ are the matrices for 16th to 25th eigentriples. Moreover, the fourth mode (mode 4) and fifth mode (mode 5) are calculated as follows:

$$\mathbf{M}_4 = \tilde{\mathbf{U}}_4 \tilde{\mathbf{S}}_4 \tilde{\mathbf{V}}_4^T \quad (6)$$

$$\mathbf{M}_5 = \tilde{\mathbf{U}}_5 \tilde{\mathbf{S}}_5 \tilde{\mathbf{V}}_5^T \quad (7)$$

where $\tilde{\mathbf{U}}_4 = \mathbf{U}(:, (26 : 40))$, $\tilde{\mathbf{S}}_4 = \mathbf{S}(:, (26 : 40), (26 : 40))$, $\tilde{\mathbf{V}}_4^T = \mathbf{V}(:, (26 : 40))$, $\tilde{\mathbf{U}}_5 = \mathbf{U}(:, (41 : 128))$,

$\tilde{\mathbf{S}}_5 = \mathbf{S}(:, (41 : 128), (41 : 128))$, and $\tilde{\mathbf{V}}_5 = \mathbf{V}(:, (41 : 128))$, respectively. Once mode 1, mode 2, mode 3, mode 4, and mode 5 are evaluated from a 12-lead ECG trace image, DRL is developed for automated detection of MI. In the SVD domain, the 12-lead ECG trace image information is crossly captured in the eigentriples. The logarithm normalized singular spectrum (LNSP) of the 12-lead ECG trace image evaluated in the SVD stage is shown in Fig. 4. It is observed that the LNSP values are different for different eigentriple cases. In this work, we have considered the fixed boundaries in the LNSP for grouping eigentriples to evaluate modes from each 12-lead ECG trace image. A different set of eigentriples fall under each boundary segment, as shown in Fig. 4. Three boundary cases, such as (5, 15, 25, 40), (5, 10, 15, 25, 40), and (5, 10, 15, 20, 25, 40), are considered to evaluate five modes, six modes, and seven modes from the SVD domain representation of the 12-lead ECG trace images. The optimal number of boundary points is evaluated using the accuracy value of the DRL network for MI detection. The unsupervised learning-based methods [25] can also be used to automatically group the eigentriples to evaluate the modes of the 12-lead ECG trace images. For six mode-based decomposition cases, mode 1, mode 2, mode 3, mode 4, mode 5, and mode 6 are extracted using (1–5), (6–10), (11–15), (16–25), (26–40), and (41–128) eigentriples of 12-lead ECG trace images. Similarly, the eigentriples based on (1–5), (6–10), (11–15), (16–20), (21–25), (26–40), and (41–128) are used for seven mode decomposition case.

C. Deep Representation Learning

The network architecture for the proposed DRL is depicted in Fig. 1. It consists of the transfer-learning-based feature extraction block, global average pooling (GAP), batch normalization (BN), dropout, and dense layers, respectively. After evaluating the modes in the eigendecomposition stage, we have considered all the five modes and the 12-lead ECG trace image as input to the EfficientNetV2B2 models [26] for extraction of features. EfficientNetV2B2 is a transfer learning model, and it uses the concept of compound scaling to uniformly scale up the depth, width, and resolution of a 12-lead ECG trace image. The EfficientNetV2B2 model has 8.7 million parameters [27]. However, in the proposed work, we have considered the weight parameters of the EfficientNetV2B2 model previously trained on the ImageNet dataset [28]. Hence, the weight parameters of the EfficientNetV2B2 model are frozen for each mode, and the number of trainable parameters is only due to the BN layer and dense layers, respectively. The size of each feature map after frozen weight EfficientNetV2B2 model is $4 \times 4 \times 1408$. In this work, we have applied GAP to reduce the spatial dimension of each feature map from $4 \times 4 \times 1408$ to 1×1408 . GAP is a dimension reduction strategy in which the size of the tensor has been reduced from $m \times n \times p$ to $1 \times p$. Each $m \times n$ feature map is mapped to only one value by considering the average of all the mn values. Mathematically, the GAP is defined by [29]

$$\tilde{\mathbf{M}}_i(1, r) = \frac{1}{mn} \sum_{j_1=1}^m \sum_{j_2=1}^n \mathbf{M}_i(j_1, j_2, r) \quad (8)$$

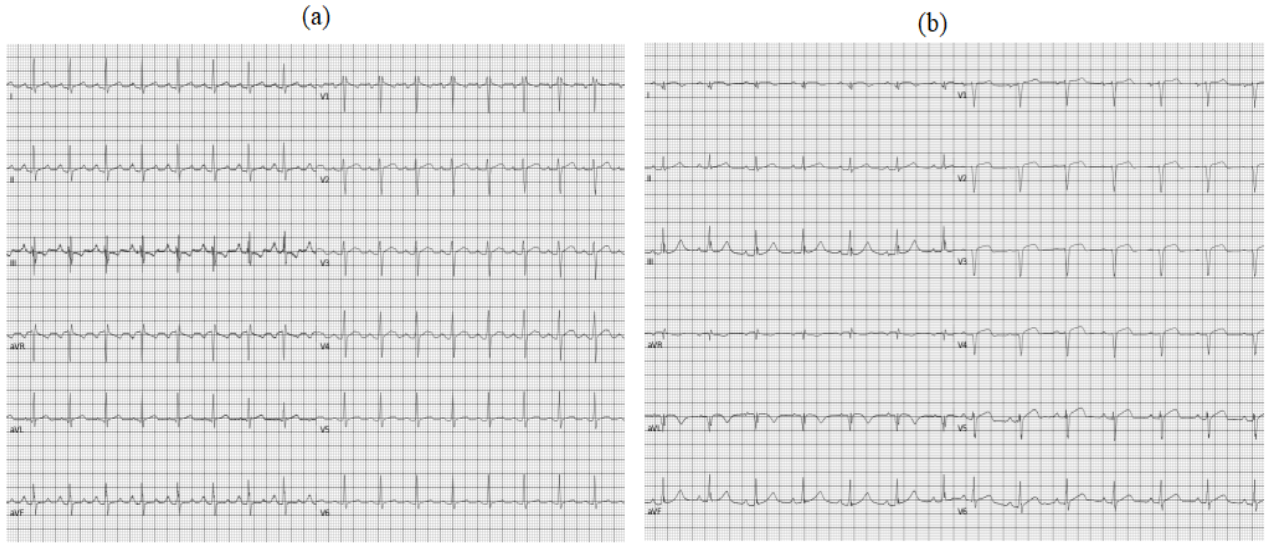


Fig. 3. (a) 12-Lead ECG trace image evaluated from the PTB database signal for normal class. (b) 12-Lead ECG trace image evaluated from the PTB database signal for MI class.

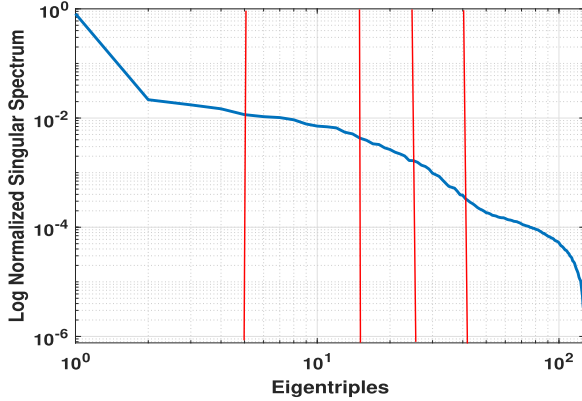


Fig. 4. LNSP plot for the 12-lead ECG trace image.

where \mathbf{M}_i is the i th feature map evaluated in the EfficientNetV2B2 stage and its size is $4 \times 4 \times 1408$. The size of $\tilde{\mathbf{M}}_i$ is $1 \times r$ for each mode and 12-lead ECG trace image itself ($r = 1408$). After the GAP layer, the BN layer is used in the proposed DRL network. The mathematical expression for the BN layer for the i th feature map is given as follows [30]:

$$\bar{\mathbf{M}}_i = \text{BN}_{\alpha, \beta}(\hat{\mathbf{M}}_i) = \alpha \hat{\mathbf{M}}_i + \beta \quad (9)$$

where α and β are the scale and shift parameters, respectively. The $\hat{\mathbf{M}}_i$ is evaluated as $\hat{\mathbf{M}}_i = (\mathbf{M}_i - \mu_b / (\sigma_b^2 + \epsilon)^{1/2})$, where μ_b and σ_b^2 are the mini-batch mean and mini-batch variance, respectively [30]. The μ_b and σ_b are calculated as $\mu_b = (1/T) \sum_{t=1}^T \mathbf{M}_i^t$ and $\sigma_b^2 = (1/T) \sum_{t=1}^T (\mathbf{M}_i^t - \mu_b)^2$, respectively. The factor T is called the mini-batch size. After the BN layer, the dropout layer is considered for the proposed network, and the dropout factor is taken to be 0.15 for each feature map. Similarly, after the dropout layer, we have considered the dense layer with three neurons and a softmax activation function for each feature map followed by feature integration or mapping. The softmax probabilities for the three classes, from each of the five modes and the preprocessed trace image, are then concatenated to form a vector of size 1×18 . Furthermore, the 18-D feature vector is then reduced to a 10-D

vector using a dense layer with rectified linear unit (ReLU) activation function. The 10-D feature vector is then given to the output layer for detecting MI and other cardiac ailments. The output layer comprises three neurons, representing normal, MI, and other cardiac ailment classes. The performance of the proposed eigendomain DRL network is compared with different transfer learning model-based frameworks for MI detection. We have considered 24 transfer learning models to evaluate the classification results for MI detection using the 12-lead ECG trace images. These baseline transfer learning models are available in the Keras and TensorFlow frameworks [31], [32]. For each transfer learning case, we have disconnected the classification or final layer in the existing model trained using the images from ImageNet. The pretrained weights of each transfer learning model are frozen, and the last layer before the output layer of the transfer learning model is used as the input to the GAP layer, BN layer, and dropout layer, followed by the classification layer (softmax activation function) containing three neurons which are interpreted as three classes such as healthy, MI, and other cardiac ailments. Fine-tuning is performed only for the weight matrix between the dropout layer and the classification (output) layer of each transfer-learning-based model for MI detection. The hold-out validation and fivefold cross-validation (CV) methods are used for the proposed DRL and different transfer learning models to select the training and test sets for MI detection using modes of 12-lead ECG trace images from both the databases. For hold-out validation, we have considered the 60%, 20%, and 20% instances of the 12-lead ECG trace images as training, validation, and testing for the proposed DRL and other transfer learning models [11]. Similarly, for fivefold CV, the 12-lead ECG trace images are divided into training and testing from different instance locations of the dataset in each fold for the DRL and transfer-learning-based models for MI detection.

The hyperparameters used to train the proposed DRL network to detect MI are the learning rate as 7.5×10^{-3} , Adam optimizer, categorical cross-entropy-based cost function, and batch size as 16. The learnable weight parameters during the

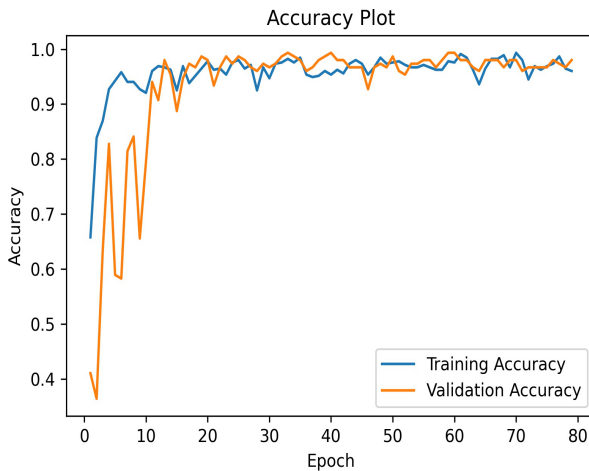


Fig. 5. Accuracy versus epoch plot using holdout CV for the proposed DRL classifier to detect MI.

training of the proposed DRL model are based on the minimization of the negative categorical cross-entropy-based cost function. The early stopping with the patience of 20 epochs is used in training the proposed DRL model. Patience is a vital parameter in early stopping cases for the training of DL models [33]. These hyperparameters are optimized using the grid-search-based method. The total trainable parameters for the proposed DRL network is approximately 42 000. The hyperparameters used for training each transfer learning model are the same as the proposed DRL model for MI detection using the 12-lead ECG trace images. In the proposed work, we have resized the 12-lead ECG trace image to [128, 128] in the SVD decomposition phase. The EfficientNetV2B2 model has considered the input as a third-order tensor. Hence, after the SVD phase, we formulated the third-order tensor [(128, 128, 3)] for each mode by appending three same grayscale representations. In the original EfficientNetV2B2-based DL model, the size of the input tensor is given as (260, 260, 3) [26]. The size of the tensor obtained in the final convolution layer of the EfficientNetV2B2 model is (9, 9, 1408) [26]. As the reduced size input tensor [(128, 128, 3)] is used for the frozen-weight-based transfer learning model, the size of feature maps produced in the different layers of this model is different from that of the original EfficientNetV2B2 model. Therefore, for the new input tensor of size (128, 128, 3), the feature map size produced at the final convolution layer is (4, 4, 1408). The DRL framework developed in Fig. 1 contains multiple EfficientNetV2B2-based transfer learning models. We have also formulated the DRL frameworks by considering ResNet50, VGG16, InceptionV3, and DenseNet121-based transfer learners in place of EfficientNetV2B2 in Fig. 1. These models are DRL based on ResNet50, DRL based on InceptionV3, DRL based on VGG16, and DRL based on DenseNet121. The performance of the DRL frameworks and each transfer learning model is evaluated using various measures such as accuracy, precision, specificity, recall, F1-score, and Kappa score, respectively [11], [34]. In this study, we have not used data augmentation as there is not much difference in the number of the 12-lead ECG trace image instances between healthy, MI, and other ailment classes.

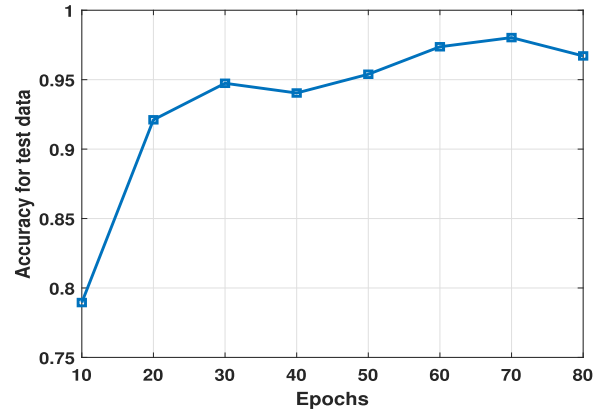


Fig. 6. Accuracy versus epoch plot of the proposed DRL model using the test 12-lead ECG trace images.

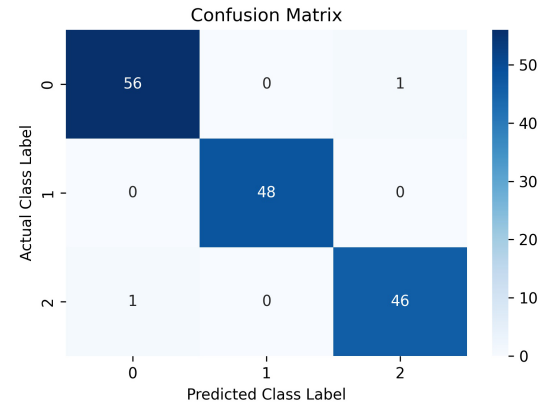


Fig. 7. Confusion matrix evaluated for the proposed DRL model for hold-out validation (0 as normal class, 1 as MI class, and 2 as other cardiac ailment class).

IV. RESULTS AND DISCUSSION

In this section, we have shown the classification performance of the proposed DRL model and 24 existing transfer-learning-based techniques to detect MI using the 12-lead ECG trace images. The accuracy versus epoch plot of the proposed DRL model for hold-out validation is shown in Fig. 5. In the case of a hold-out CV, the training accuracy increases after the 1st epoch. The validation accuracy increases steadily after the 10th epoch, and both the training and validation accuracy values are attained as 98.684% after the 80th epoch. In this work, we have used early stopping with patience of 20 epochs for the training of the DRL model. The total number of epochs is 80 for the proposed DRL model during the training phase. The patience set to 20 epochs means the training of the proposed DRL model will be terminated if both the training and validation accuracy values are not improving in the last 20 epochs. However, in the accuracy versus epoch plot shown in Fig. 5, training and validation accuracy values vary slightly after 20 epochs. Therefore, we have shown training and validation accuracy values up to 80 epochs, as the patience of 20 epochs cannot terminate the training of the proposed DRL model in the early stopping stage. The patience value can be set as below 20 epochs to reduce the search space of the DRL model during training. However, we have obtained higher accuracy values for the patience of 20 epochs in the training of the proposed DRL model. The accuracy versus epoch plot

TABLE I
CLASSIFICATION PERFORMANCE OF THE PROPOSED DRL AND DIFFERENT TRANSFER LEARNING MODELS TO DETECT MI USING 12-LEAD ECG TRACE IMAGES WITH HOLD-OUT VALIDATION

Sl. no.	Model	Accuracy(%)	Precision(%)	Recall(%)	F1 Score(%)	Specificity(%)	Kappa Score(%)
1	EfficientNetB0	96.05± 0.41	96.37± 0.41	95.84± 0.45	95.99± 0.44	97.95± 0.21	94.04± 0.62
2	EfficientNetB1	95.92± 0.64	96.06± 0.77	95.80± 0.59	95.86± 0.65	97.92± 0.30	93.85± 0.96
3	EfficientNetB2	96.31± 0.89	96.51± 0.82	96.17± 0.94	96.22± 0.94	98.13± 0.44	94.46± 1.34
4	EfficientNetB3	96.71± 1.31	97.05± 1.11	96.47± 1.43	96.61± 1.38	98.29± 0.68	95.03± 1.99
5	EfficientNetB4	96.18± 1.87	96.19± 1.89	96.07± 1.94	96.08± 1.94	98.08± 0.93	94.25± 2.83
6	EfficientNetB5	93.68± 1.35	93.70± 1.40	93.57± 1.32	93.57± 1.35	96.82± 0.66	90.48± 2.03
7	EfficientNetB6	94.60± 1.52	94.75± 1.61	94.48± 1.51	94.49± 1.55	97.30± 0.73	91.87± 2.29
8	EfficientNetB7	95.26± 1.27	95.60± 1.01	94.94± 1.39	95.01± 1.40	97.59± 0.66	92.84± 1.93
9	EfficientNetV2B0	98.15± 0.96	98.21± 0.91	98.06± 1.02	98.09± 0.98	99.07± 0.49	97.22± 1.45
10	EfficientNetV2B1	97.50± 0.26	97.83± 0.30	97.34± 0.26	97.51± 0.26	98.68± 0.13	96.22± 0.39
11	EfficientNetV2B2	98.28± 0.67	98.40± 0.68	98.23± 0.63	98.28± 0.65	99.11± 0.33	97.42± 1.00
12	EfficientNetV2B3	96.44± 1.14	96.71± 1.02	96.18± 1.22	96.33± 1.14	98.18± 0.61	94.63± 1.73
13	ResNet50	97.50± 0.96	97.68± 1.03	97.31± 1.02	97.44± 1.03	98.71± 0.47	96.22± 1.45
14	ResNet101	96.05± 1.24	96.37± 1.05	95.74± 1.34	95.84± 1.33	97.99± 0.64	94.04± 1.88
15	ResNet152	97.50± 1.27	97.53± 1.20	97.43± 1.28	97.46± 1.25	98.74± 0.65	96.23± 1.92
16	VGG16	95.52± 1.40	95.68± 1.23	95.33± 1.47	95.38± 1.39	97.74± 0.74	93.25± 2.12
17	VGG19	95.52± 1.13	95.91± 0.88	95.22± 1.25	95.33± 1.23	97.71± 0.59	93.24± 1.71
18	Xception	92.63± 1.34	93.01± 1.37	92.52± 1.21	92.50± 1.31	96.28± 0.64	88.89± 2.00
19	InceptionV3	96.05± 1.31	96.33± 1.36	96.01± 1.34	96.05± 1.38	97.98± 0.64	94.05± 1.98
20	DenseNet121	97.50± 1.46	97.71± 1.25	97.30± 1.57	97.40± 1.53	98.71± 0.76	96.22± 2.21
21	DenseNet169	97.36± 1.10	97.56± 0.99	97.16± 1.18	97.25± 1.17	98.65± 0.56	96.03± 1.66
22	DenseNet201	95.78± 0.67	96.14± 0.70	95.48± 0.73	95.59± 0.79	97.85± 0.30	93.64± 1.01
23	InceptionResNetV2	75.39± 2.44	75.37± 2.55	74.94± 2.41	74.84± 2.49	87.74± 1.17	62.95± 3.62
24	NASNetMobile	92.89± 0.64	93.14± 0.65	92.71± 0.67	92.73± 0.702	96.38± 0.32	89.28± 0.97
25	Proposed eigendomain DRL	98.68± 0.72	98.76± 0.68	98.63± 0.73	98.68± 0.72	99.32± 0.36	98.01± 1.08

TABLE II
CLASSIFICATION PERFORMANCE OF THE PROPOSED DRL AND DIFFERENT TRANSFER LEARNING MODELS TO DETECT MI USING 12-LEAD ECG TRACE IMAGES WITH FIVEFOLD VALIDATION

Sl. no.	Model	Accuracy(%)	Precision(%)	Recall(%)	F1 Score(%)	Specificity(%)	Kappa Score(%)
1	EfficientNetB0	96.47± 0.62	96.49± 0.57	96.40± 0.70	96.41± 0.66	98.22± 0.32	94.69± 0.94
2	EfficientNetB1	96.03± 0.88	96.28± 0.77	95.87± 0.93	96.00± 0.85	97.96± 0.46	94.01± 1.33
3	EfficientNetB2	95.85± 1.26	95.99± 1.25	95.67± 1.31	95.72± 1.33	97.90± 0.62	93.75± 1.90
4	EfficientNetB3	96.47± 0.73	96.70± 0.66	96.22± 0.77	96.32± 0.76	98.20± 0.38	94.68± 1.11
5	EfficientNetB4	96.03± 0.96	96.41± 0.82	95.97± 0.94	96.03± 0.96	97.98± 0.46	94.02± 1.44
6	EfficientNetB5	95.06± 0.70	95.11± 0.68	95.10± 0.82	95.00± 0.78	97.54± 0.36	92.57± 1.06
7	EfficientNetB6	94.27± 1.60	94.48± 1.73	94.06± 1.62	94.20± 1.65	97.09± 0.78	91.36± 2.40
8	EfficientNetB7	95.24± 1.01	95.52± 0.84	94.99± 1.12	95.07± 1.10	97.57± 0.52	92.82± 1.54
9	EfficientNetV2B0	97.63± 1.14	97.59± 1.27	97.46± 1.22	97.48± 1.23	98.83± 0.54	96.43± 1.72
10	EfficientNetV2B1	98.32± 1.09	98.47± 0.93	98.20± 1.20	98.28± 1.12	99.13± 0.57	97.47± 1.65
11	EfficientNetV2B2	98.68± 0.58	98.75± 0.59	98.60± 0.60	98.65± 0.61	99.32± 0.28	98.01± 0.88
12	EfficientNetV2B3	98.23± 0.73	98.31± 0.73	98.21± 0.74	98.24± 0.73	99.10± 0.37	97.34± 1.11
13	ResNet50	97.70± 0.32	97.89± 0.31	97.52± 0.35	97.64± 0.35	98.81± 0.16	96.54± 0.49
14	ResNet101	95.15± 1.57	95.59± 1.37	94.81± 1.65	94.89± 1.67	97.55± 0.79	92.68± 2.38
15	ResNet152	95.77± 0.44	95.88± 0.41	95.59± 0.48	95.65± 0.47	97.85± 0.23	93.62± 0.67
16	VGG16	97.09± 0.44	97.28± 0.45	96.94± 0.45	97.03± 0.43	98.50± 0.23	95.61± 0.67
17	VGG19	97.53± 0.76	97.71± 0.67	97.33± 0.83	97.43± 0.79	98.73± 0.39	96.27± 1.16
18	Xception	94.71± 1.27	94.88± 1.33	94.78± 1.22	94.71± 1.30	97.35± 0.61	92.04± 1.91
19	InceptionV3	94.01± 1.86	94.70± 1.65	93.62± 1.98	93.79± 1.98	96.89± 0.96	90.94± 2.82
20	DenseNet121	98.14± 0.85	98.26± 0.74	98.00± 0.92	98.07± 0.87	99.05± 0.44	97.21± 1.28
21	DenseNet169	97.44± 0.17	97.67± 0.17	97.23± 0.19	97.36± 0.18	98.68± 0.09	96.14± 0.26
22	DenseNet201	98.23± 1.27	98.46± 1.08	98.10± 1.35	98.24± 1.25	99.07± 0.67	97.34± 1.92
23	InceptionResNetV2	79.55± 1.73	79.16± 1.82	79.12± 1.83	78.98± 1.86	89.85± 0.85	69.23± 2.61
24	NASNetMobile	92.07± 0.92	92.63± 0.70	91.69± 1.00	91.71± 1.04	95.96± 0.46	88.02± 1.40
25	Proposed eigendomain DRL	99.03± 0.70	99.09± 0.68	98.96± 0.75	99.01± 0.74	99.49± 0.35	98.53± 1.06

of the proposed DRL model evaluated using test 12-lead ECG trace images for the first run of random hold-out validation is depicted in Fig. 6. It is observed that the testing accuracy is more than 98% for the 70th epoch compared with other training epochs for the DRL model to detect MI using 12-lead ECG trace images. Similarly, the confusion matrix evaluated for 20% of the test 12-lead ECG trace images using the proposed DRL model is depicted in Fig. 7. All the test 12-lead ECG trace images for the MI class are successfully predicted as MI, thereby showing the robustness of the proposed DRL

model to detect MI. Furthermore, the number of false positive values for normal and other cardiac ailments classes is only 1, as seen in the confusion matrix plot.

The classification results obtained using the proposed eigen-domain DRL network and different transfer-learning-based frameworks for detecting MI from the 12-lead ECG trace images using hold-out validation are shown in Table I. It is noted that different versions (B0, B1, B2, B3, B4, B5, B6, and B7) of the EfficientNet-based transfer learning models have obtained overall average accuracy values of less than

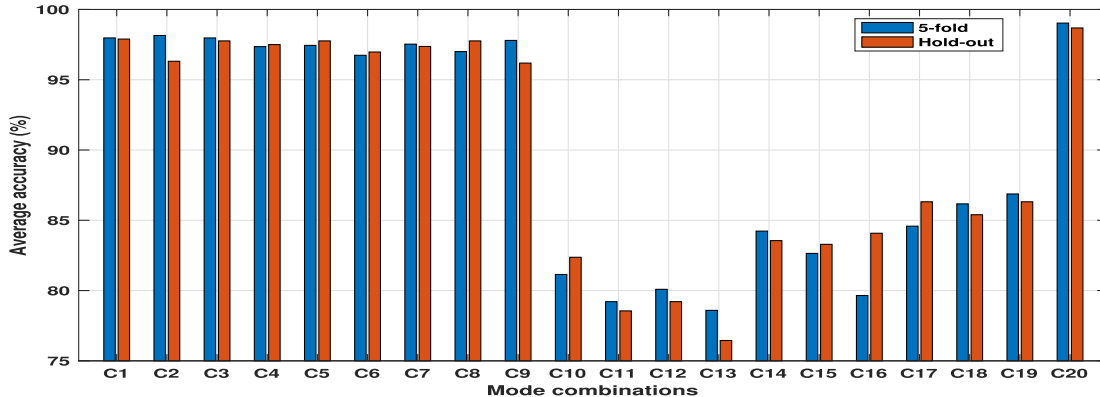


Fig. 8. Variation in the average accuracy of the proposed DRL model with different mode combinations and OGI for the 12-lead ECG trace cases. (C1: M1 + M2 + original grayscale image (OGI), C2: M2 + M3 + OGI, C3: M3 + M4 + OGI, C4: M4 + M5 + OGI, C5: M1 + M2 + M3 + OGI, C6: M2 + M3 + M4 + OGI, C7: M3 + M4 + M5 + OGI, C8: M1 + M2 + M3 + M4 + OGI, C9: M2 + M3 + M4 + M5 + OGI, C10: M1 + M2, C11: M2 + M3, C12: M3 + M4, C13: M4 + M5, C14: M1+M2 + M3, C15: M2 + M3 + M4, C16: M3 + M4 + M5, C17: M1 + M2 + M3 + M4, C18: M2 + M3 + M4 + M5, C19: M1+M2 + M3 + M4 + M5, C20: All modes and OGI).

97% for the detection of MI. Similar results are seen for F1-score, recall, and Kappa scores for different versions of the EfficientNet models. The EfficientNetB3 model has obtained higher overall accuracy than other versions of the EfficientNet-based transfer learning models for MI detection using the 12-lead ECG trace images. Furthermore, the hybrid EfficientNet models such as EfficientNetV2B0, EfficientNetV2B1, EfficientNetV2B2, and EfficientNetV2B3 have obtained more than 96% accuracy, precision, recall, and F1-score values for MI detection using the 12-lead ECG trace images. The EfficientNetV2B2 model has produced an overall average accuracy value of 98.28% when compared with all other versions of the hybrid EfficientNet models. The InceptionResNetV2-based transfer learning model has the lowest classification performance compared with other transfer learning models. Moreover, ResNet50 and ResNet 152 have obtained average accuracy values of 97.50% compared with ResNet101, VGG16, and VGG19-based transfer learning models. The proposed eigendomain DRL network has achieved the highest overall classification performance compared with EfficientNetV2B2 and other transfer learning models to detect MI using the 12-lead ECG trace images.

The results evaluated using the proposed eigendomain DRL network and the existing transfer learning models for fivefold CV are shown in Table II. It is noted that all the EfficientNet versions of the transfer learning models have achieved accuracy, recall, F1-score, and Kappa score values of less than 96.5%. The EfficientNetB3 model has a precision value of 96.70% when compared with the other versions of the EfficientNet-based transfer learning models. Furthermore, for the EfficientNetB0 model, the highest specificity value is observed compared with other EfficientNet models to detect MI using the 12-lead ECG trace images. It is also seen that the ResNet50 model has obtained higher classification results in terms of all the measures when compared with other ResNet-based transfer learning models. Similarly, the VGG16 and VGG19 models have demonstrated average accuracy values of more than 97% for fivefold CV. DenseNet121 and DenseNet201 have produced higher classification performance than Xception- and InceptionV3-based transfer learning

models. The InceptionResNetV2 model has obtained the lowest average classification accuracy and other measures compared with other transfer learning models to detect MI using the 12-lead ECG trace images. The proposed eigendomain DRL framework has obtained the highest classification performance in terms of all the metrics when compared with all the transfer learning models for fivefold CV.

In Fig. 8, we have shown the average classification accuracy of the proposed DRL model using different mode combinations and grayscale 12-lead ECG images. It is seen that when all the five modes are used, the DRL framework has produced the average accuracy values of 86.87% and 86.31% for fivefold CV and hold-out validation, respectively. Similarly, when mode 2 to mode 5 of the 12-lead ECG trace image are used, the average accuracy value of the proposed DRL model is reduced to 84.51% for the fivefold CV when compared with the first four modes case. The eigentriples obtained in the SVD phase capture signal and noise subspace information of the 12-lead ECG trace image. The accuracy value of DRL with M1 + M2 + original grayscale image (OGI) is higher than DRL with M1 + M2 + M3 + OGI and DRL with M1 + M2 + M4 + OGI for MI detection. The hidden layers in the proposed DRL model select relevant discriminative information from M1, M2, and OGI, demonstrating higher accuracy for MI detection. On the other hand, the DRL with M1 + M2 + M3 + OGI and DRL with M1 + M2 + M3 + M4 + OGI models capture noise information along with relevant signal subspace information. Due to this reason, these two models have produced lower accuracy than the DRL with M1 + M2 + OGI model for MI detection. Moreover, we have also evaluated the accuracy value of DRL with M1 + M2 + M5 + OGI model for MI detection using hold-out validation. The average accuracy value obtained using DRL with M1 + M2 + M5 + OGI model is 97.50%. It is observed that the classification performance of DRL with M1 + M2 + M5 + OGI model is lower than DRL with M1 + M2 + OGI, DRL with M1 + M2 + M3 + OGI and DRL with M1 + M2 + M3 + M4 + OGI models for MI detection using the 12-lead ECG trace images. When all the five modes and OGI are used, the DRL model has produced

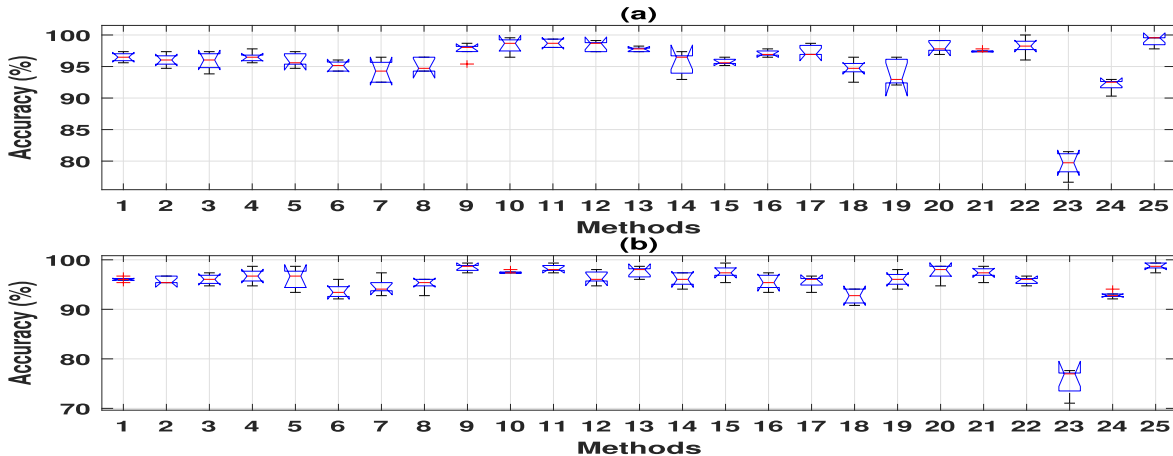


Fig. 9. (a) Boxplot showing the variations in the accuracy value of the proposed DRL approach and the existing transfer learning models for different random hold-out validation. (b) Boxplot showing the variations in the accuracy value of the proposed DRL approach and the existing transfer learning models for fivefold CV. (The serial numbers of all the methods are given in Tables I and II for hold-out validation and fivefold CV, respectively).

TABLE III

VARIATIONS IN CLASSIFICATION RESULTS OF THE PROPOSED EIGENDOMAIN DRL MODEL WITH DIFFERENT SIZES OF 12-LEAD ECG TRACE IMAGES

Size of 12-lead ECG images	Accuracy(%)	Precision(%)	Recall(%)	Specificity(%)	F1-score(%)	Kappa score(%)
[64, 64]	94.73 \pm 2.16	95.09 \pm 1.82	94.40 \pm 2.29	97.34 \pm 1.14	94.49 \pm 2.18	92.05 \pm 3.28
[128, 128]	98.68 \pm 0.72	98.76 \pm 0.68	98.63 \pm 0.73	99.32 \pm 0.36	98.68 \pm 0.72	98.01 \pm 1.08
[256, 256]	96.18 \pm 5.05	96.25 \pm 5.06	96.11 \pm 5.12	98.05 \pm 2.57	96.11 \pm 5.17	94.24 \pm 7.63

more than 99% accuracy, which is higher than other mode combinations for detecting MI. The proposed DRL model uses both local information (modes) and global information (OGI itself) of the 12-lead ECG trace images to achieve better accuracy for the automated detection of MI disease.

The Kruskal–Wallis (KW) test [35] is performed to check the significant differences in the classification accuracy values between the proposed eigendomain DRL model and the existing transfer learning models. We have executed the proposed eigendomain DRL and the existing transfer learning model five times for hold-out validation and performed the KW test. The variations in the accuracy values for all the 25 models are depicted in Fig. 9(a) and (b) for hold-out validation and fivefold CV scenarios for the detection of MI. For the fivefold CV case, the KW test is performed by considering the accuracy values of all fivefolds for the proposed model and all the 24 transfer learning models. It is noteworthy to say that the average accuracy values of the proposed model (serial number 25) are 98.68% and 99.03% for hold-out validation and fivefold CV cases, respectively. The *p*-value obtained from the KW test for hold-out validation for all the 25 models (the proposed model and all the existing 24 transfer learning models) is 1.38×10^{-10} . The small *p*-value signifies that the differences in the classification accuracy values are obtained as statistically significant between the proposed eigendomain DRL network and the existing transfer learning-based techniques. Furthermore, the *p*-value computed from the KW test for the accuracy values of all the 25 models with fivefold CV is given as 1.64×10^{-8} . Hence, the *p*-value <0.001 reveals a significant difference in the accuracy values between the proposed model and all the transfer learning models for detecting MI using the 12-lead ECG trace images.

In Fig. 10, we have compared the classification accuracy values of non-DRL (transfer learning) and DRL-based models

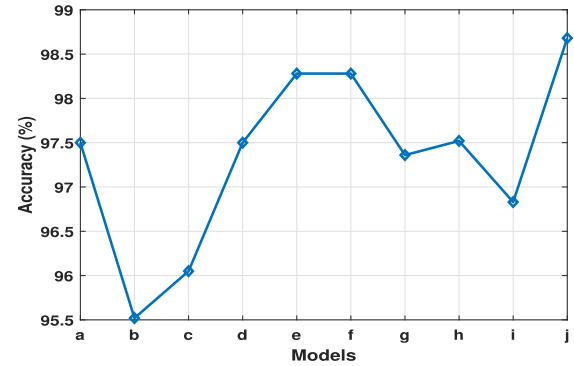


Fig. 10. Classification accuracy values of different models for MI detection using the 12-lead ECG trace images with hold-out validation (a. ResNet50, b. VGG16, c. InceptionV3, d. DenseNet121, e. EfficientNetV2B2, f. DRL based on ResNet50, g. DRL based on VGG16, h. DRL based on DenseNet121, i. DRL based on InceptionV3, j. DRL based on EfficientNetV2B2).

TABLE IV

ACCURACY VALUES OF THE PROPOSED DRL MODELS USING DIFFERENT MODES OF 12-LEAD ECG TRACE IMAGES

Mode selection	Accuracy (%)
5 modes and OGI	98.68
6 modes and OGI	98.62
7 modes and OGI	98.67

for automated MI detection with hold-out validation. It is observed that the accuracy of DRL based on ResNet50 is higher than DRL based on InceptionV3, DRL based on VGG16, and DRL based on DenseNet121 frameworks for MI detection using hold-out validation. Similarly, the accuracy values of all the DRL models are higher than the non-DRL-based models for MI detection. The proposed approach (DRL based on EfficientNetV2B2) has obtained an accuracy value of 98.68% which is the highest compared with the other DRL and non-DRL models for MI detection using the 12-lead ECG trace images. The variation in performance metrics of

TABLE V
CLASSIFICATION RESULTS OF THE PROPOSED DRL MODEL USING 12-LEAD ECG TRACE IMAGES EXTRACTED FROM THE PTB DATABASE TO DETECT MI

Validation	Accuracy (%)	Precision (%)	Recall (%)	Specificity (%)	F1-score (%)	Kappa score
Hold-out	99.88 \pm 0.23	99.86 \pm 0.27	99.90 \pm 0.20	99.90 \pm 0.20	99.88 \pm 0.23	0.997 \pm 0.47
5-fold CV	99.92 \pm 0.15	99.09 \pm 0.18	99.93 \pm 0.13	99.93 \pm 0.13	99.92 \pm 0.15	0.998 \pm 0.31

TABLE VI
COMPARISON WITH VARIOUS EXISTING METHODS FOR MI DETECTION USING 12-LEAD ECG

Methods	Input used	Accuracy (%)
11-layer 2D deep CNN model [5]	12-lead ECG trace images	86.21
Fine-tuned MobileNet model [12]	12-lead ECG trace images	95.00
Fine-tuned VGG16 model [12]	12-lead ECG trace images	95.00
CNN and BiGRU-based deep learning model [36]	12-lead ECG signals	95.76
Multiscale energy and eigenvalue features and SVM classifier [2]	12-lead ECG signals	96.00
Multiscale higher order singular value-based features and SVM classifier [37]	12-lead ECG signals	95.30
Features evaluated based on polynomial coefficients of ST-segment of each ECG lead, and multi-instance learning classifier [38]	12-lead ECG signals	90.00
Features evaluated using phase space fractal dimension of 12-lead ECG and multilayer perceptron (MLP) model [39]	12-lead ECG signals	96.00
Proposed eigendomain DRL approach	12-lead ECG trace images	98.68

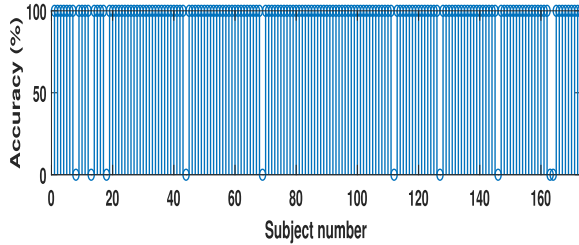


Fig. 11. LOOCV-based classification results of the proposed eigendomain DRL model using the 12-lead ECG trace images evaluated from the PTB database signals.

the proposed eigendomain DRL model with different sizes of 12-lead ECG trace images is shown in Table III. It is noted that when [64, 64] size-based 12-lead ECG trace images are considered, the suggested approach has demonstrated accuracy, precision, recall, Kappa score, and F1-score values of below 95.50%. However, the specificity value of the DRL model is obtained as 97.34%. Similarly, when the [256, 256] size-based 12-lead ECG trace images are used, the proposed approach has produced the overall accuracy, specificity, and precision values of 96.18%, 98.05%, and 96.25%, respectively. The proposed eigendomain DRL model has obtained the highest classification performance concerning all the metrics using [128, 128] size-based 12-lead ECG trace images. Moreover, we have evaluated the classification accuracy values of the proposed DRL model with six-mode- and seven-modes-based decomposition of the 12-lead trace image cases for MI detection with hold-out validation. These results are shown in Table IV. It is observed that the DRL model has obtained overall accuracy values of 98.62% and 98.67%, respectively, for six modes with OGI and seven modes with OGI. The DRL model with five modes and OGI has demonstrated the highest accuracy compared with six-mode and seven-mode cases for MI detection.

We have evaluated the classification results of the proposed eigendomain DRL framework using the 12-lead ECG trace images computed from the PTB database for MI detection. These results are depicted in Table V for both the hold-out validation and fivefold CV methods. It is observed that for

the hold-out validation case, the eigendomain DRL model has obtained an average accuracy value of more than 99.50% for MI detection using the 12-lead ECG trace images extracted from the PTB database. Similar variations have been observed in other measures of the DRL model for MI detection using a hold-out validation scheme. It is also seen that the proposed eigendomain DRL model has obtained an overall accuracy value of 99.92% to detect MI using a fivefold CV scheme. The classification performance of the eigendomain DRL model is also evaluated using the 12-lead ECG trace images computed from the PTB database with subject independent leave-one-out CV (LOOCV) scheme. The accuracy of each subject obtained using LOOCV is shown in Fig. 11. It is observed that the proposed approach has correctly classified 163 out of 173 subject's 12-lead ECG trace images. The overall accuracy for LOOCV is obtained as 94.21%. The higher accuracy in all the three validation methods reveals that the proposed eigendomain DRL model successfully detects MI disease using the 12-lead ECG trace images of different formats.

We have compared the classification accuracy of the proposed eigendomain DRL approach with different existing methods in Table VI to detect MI using the 12-lead ECG. The 11-layer deep CNN model reported in [5] has higher trainable parameters than the proposed DRL model for MI detection. It is also observed that the accuracy of the 11-layer deep CNN model is less than the proposed approach to detect MI using the 12-lead ECG trace images. Similarly, the fine-tuned MobileNet-based transfer learning model has obtained an accuracy value of 95%, and the number of trainable parameters is 2 888 708. The fine-tuned VGG model has obtained an accuracy value of 95%, and the number of training parameters is 26 480 644. The proposed eigendomain DRL model has obtained an accuracy value of 98.68% and has 42 481 as the number of trainable parameters. Furthermore, we have also compared the classification results of the proposed eigendomain DRL approach with the existing 12-lead ECG signal-based methods for MI detection. Fu et al. [36], have used CNN and bidirectional gated recurrent unit (BiGRU)-based DL model to detect MI using the 12-lead ECG signals and reported an accuracy value of 95.76%. Similarly, the wavelet-based

multiscale domain methods have obtained accuracy values of 96% and 95.30%, respectively, for MI detection using the 12-lead ECG signals [2], [37]. The polynomial-coefficient-based features from the ST-segment of the 12-lead ECG signals coupled with a multiinstance learning-based model have demonstrated the average accuracy value of 90% to detect MI [38]. Similarly, Lahiri et al. [39] have used the phase space-based fractional dimension features of the 12-lead ECG signals and multilayer perceptron (MLP) classifier to detect MI. The proposed approach has shown higher accuracy in detecting MI using different existing 12-lead ECG trace images and 12-lead ECG signal-based methods. The 12-lead ECG signal-based methods require various preprocessing tasks such as removing artifacts, beat segmentation, feature extraction, feature selection, and using classifiers to detect MI. Similarly, the DL model using the 12-lead ECG signals has higher trainable parameters for MI detection. The proposed eigendomain DRL model has fewer trainable parameters than the methods in [5], [12], and [36] for MI detection using the 12-lead ECG. Therefore, the proposed model is lightweight, computationally easy to train, and accurate in detecting MI using the 12-lead ECG trace images. The proposed work has the following advantages, which are given below.

- 1) The eigenanalysis and grouping are used to obtain modes or local diagnostic information from the 12-lead ECG trace images.
- 2) The proposed DRL network uses the original 12-lead ECG trace image information and eigendomain modes' information to detect MI.
- 3) The proposed eigendomain DRL model has demonstrated supreme performance than the existing transfer learning models for normal versus MI versus other cardiac ailment classification tasks using the 12-lead trace images.
- 4) The differences in the overall accuracy values are found as significant from the statistical tests.
- 5) The proposed eigendomain DRL approach does not require R-peak identification and other processing techniques such as the 12-lead ECG signal-based methods to detect MI.

In ECG, symptoms such as T-wave inversion, ST-segment elevation, and abnormal Q-wave are typically used for diagnosing MI disease [2]. These pathological changes are seen in different lead sets for different types of MI. The long bottom lead in the first format 12-lead ECG trace image in Fig. 2 helps observe the variations in more than three beats of only lead II ECG data for MI detection. Similarly, the second format 12-lead trace image shown in Fig. 3 captures more than five beats of information on each ECG lead. The proposed DRL model has obtained more than 98% accuracy using two different formats based on the 12-lead ECG trace images for MI detection. In this work, we have used an ECG-plot-based existing python library [24] to synthesize the 12-lead ECG trace images from the PTB database ECG signals. In the future, the software program to synthesize the 12-lead ECG trace image as close to Fig. 2 with different bottom leads can be implemented to evaluate the performance

of the proposed DRL model to detect MI. We have considered the 12-lead ECG trace images from normal, MI, and other cardiac ailments in the present work to develop the proposed eigendomain DRL model. MI localization, such as classifying different types of MI such as anterior, posterior, inferior, and lateral MI [40], [41], can be performed using the proposed eigendomain DRL model with the 12-lead ECG trace images. Similarly, novel DL-based models can be developed to automatically detect atrial flutter, atrial fibrillation (AF), paroxysmal AF, and persistent AF [42] using the 12-lead ECG trace images.

V. CONCLUSION

The eigendomain DRL framework has been proposed to automatically detect MI using the 12-lead ECG trace images. The SVD and eigentriple grouping has been used to obtain the modes or components from the 12-lead ECG trace images. The DRL network uses original grayscale 12-lead ECG images and all the modes of information to detect MI disease. The proposed approach has demonstrated higher classification results in various performance metrics for the classification of normal versus MI versus other cardiac ailments compared with 24 different transfer learning techniques. For the MI class, the suggested approach has been produced with 100% accuracy using the global and local information of the 12-lead ECG trace images. From the statistical perspective, it has been verified that the difference in the accuracy measures between the proposed eigendomain DRL network and other transfer learning models is significant. In the future, the proposed approach can be used to localize various types of MI and other cardiac ailments using the 12-lead ECG trace images.

REFERENCES

- [1] M. Caldwell, L. Martinez, J. G. Foster, D. Sherling, and C. H. Hennekens, "Prospects for the primary prevention of myocardial infarction and stroke," *J. Cardiovascular Pharmacol. Therapeutics*, vol. 24, no. 3, pp. 207–214, May 2019.
- [2] L. N. Sharma, R. K. Tripathy, and S. Dandapat, "Multiscale energy and eigenspace approach to detection and localization of myocardial infarction," *IEEE Trans. Biomed. Eng.*, vol. 62, no. 7, pp. 1827–1837, Jul. 2015.
- [3] D. Sadhukhan, S. Pal, and M. Mitra, "Automated identification of myocardial infarction using harmonic phase distribution pattern of ECG data," *IEEE Trans. Instrum. Meas.*, vol. 67, no. 10, pp. 2303–2313, Oct. 2018.
- [4] R. K. Tripathy and S. Dandapat, "Detection of myocardial infarction from vectorcardiogram using relevance vector machine," *Signal, Image Video Process.*, vol. 11, no. 6, pp. 1139–1146, 2017.
- [5] R. K. S. Sane, P. S. Choudhary, L. N. Sharma, and P. S. Dandapat, "Detection of myocardial infarction from 12 lead ECG images," in *Proc. Nat. Conf. Commun. (NCC)*, Jul. 2021, pp. 1–6.
- [6] D. M. Mirvis and A. L. Goldberger, "Electrocardiography," *Heart Disease*, vol. 1, pp. 82–128, Jan. 2001.
- [7] R. K. Tripathy, A. Bhattacharyya, and R. B. Pachori, "A novel approach for detection of myocardial infarction from ECG signals of multiple electrodes," *IEEE Sensors J.*, vol. 19, no. 2, pp. 4509–4517, Jun. 2019.
- [8] K. Mischke et al., "Telephonic transmission of 12-lead electrocardiograms during acute myocardial infarction," *J. Telemed. Telecare*, vol. 11, no. 4, pp. 185–190, 2005.
- [9] G. Al Hinai, S. Jammoul, Z. Vajjhi, and J. Afilalo, "Deep learning analysis of resting electrocardiograms for the detection of myocardial dysfunction, hypertrophy, and ischaemia: A systematic review," *Eur. Heart J.-Digit. Health*, vol. 2, no. 3, pp. 416–423, Sep. 2021.
- [10] D. Dai, L. Yu, and H. Wei, "Parameters sharing in residual neural networks," *Neural Process. Lett.*, vol. 51, no. 2, pp. 1393–1410, Apr. 2020.

- [11] J. Karhade, S. Dash, S. K. Ghosh, D. K. Dash, and R. K. Tripathy, "Time-frequency-Domain deep learning framework for the automated detection of heart valve disorders using PCG signals," *IEEE Trans. Instrum. Meas.*, vol. 71, pp. 1–11, 2022.
- [12] L. Mhamdi, O. Dammak, F. Cottin, and I. B. Dhaou, "Artificial intelligence for cardiac diseases diagnosis and prediction using ECG images on embedded systems," *Biomedicines*, vol. 10, no. 8, p. 2013, Aug. 2022.
- [13] E. Irmak, "COVID-19 disease diagnosis from paper-based ECG trace image data using a novel convolutional neural network model," *Phys. Eng. Sci. Med.*, vol. 45, no. 1, pp. 167–179, Mar. 2022.
- [14] O. Attallah, "ECG-BiCoNet: An ECG-based pipeline for COVID-19 diagnosis using bi-layers of deep features integration," *Comput. Biol. Med.*, vol. 142, Mar. 2022, Art. no. 105210.
- [15] T. Rahman et al., "COV-ECGNET: COVID-19 detection using ECG trace images with deep convolutional neural network," *Health Inf. Sci. Syst.*, vol. 10, no. 1, pp. 1–16, 2022.
- [16] N. Muralidharan, S. Gupta, M. R. Prusty, and R. K. Tripathy, "Detection of COVID19 from X-ray images using multiscale deep convolutional neural network," *Appl. Soft Comput.*, vol. 119, Apr. 2022, Art. no. 108610.
- [17] M. E. Wall, A. Rechtsteiner, and L. M. Rocha, "Singular value decomposition and principal component analysis," in *A Practical Approach to Microarray Data Analysis*. Cham, Switzerland: Springer, 2003, pp. 91–109.
- [18] R. K. Tripathy and S. Dandapat, "Multiresolution inter-sample and interlead eigen error features for classification of cardiac diseases," in *Proc. 22nd Nat. Conf. Commun. (NCC)*, Mar. 2016, pp. 1–4.
- [19] H. Yao, S. Zhang, R. Hong, Y. Zhang, C. Xu, and Q. Tian, "Deep representation learning with part loss for person re-identification," *IEEE Trans. Image Process.*, vol. 28, no. 6, pp. 2860–2871, Jun. 2019.
- [20] C. Nagpal, X. Li, and A. Dubrawski, "Deep survival machines: Fully parametric survival regression and representation learning for censored data with competing risks," *IEEE J. Biomed. Health Informat.*, vol. 25, no. 8, pp. 3163–3175, Aug. 2021.
- [21] A. H. Khan and M. Hussain, "ECG images dataset of cardiac patients," Univ. Manage. Technol., Lahore, Pakistan, Tech. Rep. 106762, 2021, doi: [10.17632/GWBZ3FSGP8.2](https://doi.org/10.17632/GWBZ3FSGP8.2).
- [22] R. Bousseljot, D. Kreiseler, and A. Schnabel, "Nutzung der EKG-Signalbank CARDIODAT der PTB über das internet," Walter de Gruyter, Berlin, Germany, Tech. Rep. 317, 1995.
- [23] A. L. Goldberger et al., "PhysioBank, PhysioToolkit, and PhysioNet: Components of a new research resource for complex physiologic signals," *Circulation*, vol. 101, no. 23, pp. e215–e220, 2000.
- [24] *ECG-Plot*. Accessed: Nov. 5, 2022. [Online]. Available: <https://pypi.org/project/ecg-plot/>
- [25] J. Harmouche, D. Fourer, F. Auger, P. Borgnat, and P. Flandrin, "The sliding singular spectrum analysis: A data-driven nonstationary signal decomposition tool," *IEEE Trans. Signal Process.*, vol. 66, no. 1, pp. 251–263, Jan. 2018.
- [26] M. Tan and Q. Le, "EfficientNetV2: Smaller models and faster training," in *Proc. Int. Conf. Mach. Learn.*, 2021, pp. 10096–10106.
- [27] M. Tan and Q. Le, "EfficientNet: Rethinking model scaling for convolutional neural networks," in *Proc. Int. Conf. Mach. Learn.*, 2019, pp. 6105–6114.
- [28] J. Deng, W. Dong, R. Socher, L.-J. Li, K. Li, and L. Fei-Fei, "ImageNet: A large-scale hierarchical image database," in *Proc. IEEE Conf. Comput. Vis. Pattern Recognit.*, Jun. 2009, pp. 248–255.
- [29] Z. Li, S.-H. Wang, R.-R. Fan, G. Cao, Y.-D. Zhang, and T. Guo, "Teeth category classification via seven-layer deep convolutional neural network with max pooling and global average pooling," *Int. J. Imag. Syst. Technol.*, vol. 29, no. 4, pp. 577–583, May 2019.
- [30] N. Bjorck, C. P. Gomes, B. Selman, and K. Q. Weinberger, "Understanding batch normalization," in *Proc. Adv. Neural Inf. Process. Syst.*, vol. 31, 2018, pp. 1–15.
- [31] *Keras Transfer Learning Models*. Accessed: Jun. 15, 2022. [Online]. Available: <https://keras.io/api/applications/>
- [32] D. Sarkar, R. Bali, and T. Ghosh, *Hands-on Transfer Learning With Python: Implement Advanced Deep Learning and Neural Network Models Using TensorFlow and Keras*. Birmingham, U.K.: Packt Publishing Ltd, 2018.
- [33] P. Nevavuori, N. Narra, and T. Lipping, "Crop yield prediction with deep convolutional neural networks," *Comput. Electron. Agricult.*, vol. 163, Aug. 2019, Art. no. 104859.
- [34] J. Quinn, J. McEachen, M. Fullan, M. Gardner, and M. Drummy, *Dive Into Deep Learning: Tools for Engagement*. Thousand Oaks, CA, USA: Corwin Press, 2019.
- [35] P. E. McKnight and J. Najab, "Kruskal-Wallis test," in *The Corsini Encyclopedia of Psychology*. Hoboken, NJ, USA: Wiley, 2010.
- [36] L. Fu, B. Lu, B. Nie, Z. Peng, H. Liu, and X. Pi, "Hybrid network with attention mechanism for detection and location of myocardial infarction based on 12-lead electrocardiogram signals," *Sensors*, vol. 20, no. 4, p. 1020, Feb. 2020.
- [37] S. Padhy and S. Dandapat, "Third-order tensor based analysis of multilead ECG for classification of myocardial infarction," *Biomed. Signal Process. Control*, vol. 31, pp. 71–78, Jan. 2017.
- [38] L. Sun, Y. Lu, K. Yang, and S. Li, "ECG analysis using multiple instance learning for myocardial infarction detection," *IEEE Trans. Biomed. Eng.*, vol. 59, no. 12, pp. 3348–3356, Dec. 2012.
- [39] T. Lahiri, U. Kumar, H. Mishra, S. Sarkar, and A. D. Roy, "Analysis of ECG signal by chaos principle to help automatic diagnosis of myocardial infarction," CSIR, Bihar, India, Tech. Rep. 68, 2009.
- [40] R. K. Tripathy, A. Bhattacharyya, and R. B. Pachori, "Localization of myocardial infarction from multi-lead ECG signals using multiscale analysis and convolutional neural network," *IEEE Sensors J.*, vol. 19, no. 23, pp. 11437–11448, Dec. 2019.
- [41] J. Zhang et al., "Automated localization of myocardial infarction of image-based multilead ECG tensor with tucker2 decomposition," *IEEE Trans. Instrum. Meas.*, vol. 71, pp. 1–15, 2021.
- [42] T. Radhakrishnan, J. Karhade, S. K. Ghosh, P. R. Muduli, R. K. Tripathy, and U. R. Acharya, "AFCNNNet: Automated detection of AF using chirplet transform and deep convolutional bidirectional long short term memory network with ECG signals," *Comput. Biol. Med.*, vol. 137, Oct. 2021, Art. no. 104783.